



## Nanoplastics affect moulting and faecal pellet sinking in Antarctic krill (*Euphausia superba*) juveniles

E. Bergami<sup>a,\*</sup>, C. Manno<sup>b</sup>, S. Cappello<sup>c</sup>, M.L. Vannuccini<sup>a</sup>, I. Corsi<sup>a</sup>

<sup>a</sup> Department of Physical, Earth and Environmental Sciences (DSFTA), University of Siena, Siena 53100, Italy

<sup>b</sup> British Antarctic Survey (BAS), Natural Environment Research Council, Cambridge CB3 0ET, UK

<sup>c</sup> Institute for Biological Resources and Marine Biotechnologies (IRBIM), National Research Council, Messina 98121, Italy



### ARTICLE INFO

Handling Editor: Adrian Covaci

#### Keywords:

Antarctic krill  
Southern Ocean  
Nanoplastics  
Polystyrene nanoparticles  
Faecal pellets  
Carbon export

### ABSTRACT

Plastic debris has been identified as a potential threat to Antarctic marine ecosystems, however, the impact of nanoplastics ( $< 1 \mu\text{m}$ ) is currently unexplored. Antarctic krill (*Euphausia superba*) is a keystone species of Southern Ocean pelagic ecosystems, which plays a central role in the Antarctic food webs and carbon (C) cycle. Krill has been shown to rapidly fragment microplastic beads through the digestive system, releasing nanoplastics with unknown toxicological effects. Here we exposed krill juveniles to carboxylic ( $-\text{COOH}$ , anionic) and amino ( $-\text{NH}_2$ , cationic) polystyrene nanoparticles (PS NPs) and we investigated lethal and sub-lethal endpoints after 48 h. The analysis of PS NP suspensions in Antarctic sea water (SW) media showed that PS-COOH formed large agglomerates ( $1043 \pm 121 \text{ nm}$ ), while PS-NH<sub>2</sub> kept their nominal size ( $56.8 \pm 3 \text{ nm}$ ) during the exposure time. After 48 h, no mortality was found but increase in exuviae production ( $12.6 \pm 1.3\%$ ) and reduced swimming activity were observed in juveniles exposed to PS-NH<sub>2</sub>. The microbial community composition in SW supports the release of krill moults upon PS NP exposure and stimulates further research on the pivotal role of krill in shaping Southern Ocean bacterial assemblages. The presence of fluorescent signal in krill faecal pellets (FPs) confirmed the waterborne ingestion and egestion of PS-COOH at 48 h of exposure. Changes in FP structure and properties were also associated to the incorporation of PS NPs regardless of their surface charge. The effects of PS NPs on krill FP properties were compared to Control 0 h as a reference for full FPs (plastic vs food) and Control 48 h as a reference for more empty-like FPs (plastic vs lack of food). Exposure to PS NPs led to a FP sinking rate comparable to Control 48 h, but significantly lower than Control 0 h ( $58.40 \pm 23.60 \text{ m/d}$  and  $51.23 \pm 28.60 \text{ m/d}$  for PS-COOH and PS-NH<sub>2</sub>;  $168.80 \pm 74.58 \text{ m/d}$  for Control 0 h). Considering the important role played by krill in the food web and C export in the Southern Ocean, the present study provides cues about the potential impact of nanoplastics on Antarctic pelagic ecosystems and their biogeochemical cycles.

### 1. Introduction

Marine plastic pollution has reached the most remote regions on Earth, including deep-sea (Chiba et al., 2018; Jamieson et al., 2019), Arctic sea ice (Obbard et al., 2014; Peeken et al., 2018) and Antarctica (Suaria et al., 2020). Once at sea, macroplastics ( $> 1 \text{ cm}$ ) are exposed to weathering agents and undergo inevitable breakdown into small fragments (Andrady, 2017, 2011) down to micro- and nano-sized debris ( $< 1 \text{ mm}$  and  $< 1 \mu\text{m}$ , respectively) (Hartmann et al., 2019). Nanoplastics occurrence and/or formation in the oceans was first hypothesised based on the loss of plastics in surface waters (Cózar et al., 2014), modelling (Kooi et al., 2017) and more recently confirmed in the North Atlantic sub-tropical gyre and Mediterranean Sea by *ad hoc* analytical methods (Schirrinzi et al., 2019; Ter Halle et al., 2017).

The occurrence of nanoplastic pollution in the Southern Ocean is currently unexplored but the documented presence of macro- and microplastics in surface waters (Jones-Williams et al., 2020; Lacerda et al., 2019; Suaria et al., 2020), sediments (Munari et al., 2017; Reed et al., 2018) and marine species (Bessa et al., 2019; Le Guen et al., 2020; Phillips and Waluda, 2020; Sfriso et al., 2020) raises concerns over the potential impact of the smallest plastic particles. Dawson et al. (2018a) recently demonstrated the ability of Antarctic krill (*Euphausia superba*, henceforth referred to as krill) to fragment ingested polyethylene microplastics (PE MPs) into nanoplastics, which were found in the egested faecal pellets (FPs).

Due to their large surface area to volume ratio, nanoplastics can follow the same route of cellular uptake of natural and engineered nanoparticles (e.g. phagocytosis, endocytosis, direct trans-membrane

\* Corresponding author at: Department of Physical, Earth and Environmental Sciences, University of Siena, Via P. A. Mattioli 4, Siena 53100, Italy.

E-mail address: [elisa.bergami@unisi.it](mailto:elisa.bergami@unisi.it) (E. Bergami).

<https://doi.org/10.1016/j.envint.2020.105999>

Received 19 February 2020; Received in revised form 17 July 2020; Accepted 17 July 2020

0160-4120/© 2020 Published by Elsevier Ltd. This is an open access article under the CC BY-NC-ND license (<http://creativecommons.org/licenses/by-nc-nd/4.0/>).

transport, etc) and once internalised in the cell they can interact with organelles and DNA, causing severe damage and cell death (Blasco and Corsi, 2019). Model nanoplastics, such as charged polystyrene nanoparticles (PS NPs), have been largely tested to investigate their ecotoxicity in marine planktonic species (Cole and Galloway, 2015; Della Torre et al., 2014; Varó et al., 2019), associated to their nano-specific features and functionalization as well as their behaviour in sea water (SW). Negatively charged PS NPs, such as carboxylic-modified (–COOH) NPs, rapidly agglomerate in SW media characterised by high ionic strength due to interactions with ionic species, in particular divalent cations (e.g.  $\text{Ca}^{2+}$ ,  $\text{Mg}^{2+}$ ) (Cai et al., 2018), which facilitate bridging effect between nanoplastics and natural organic matter (NOM) leading to NP instability (Singh et al., 2019). Thus, PS-COOH can easily be ingested/egested in the organisms in the micrometre range. On the contrary, positively charged PS NPs, such as amino-modified (–NH<sub>2</sub>) NPs, usually maintain their nano-dimension and high reactivity, which favour the interaction with biological surfaces according to the “proton sponge” hypothesis (Nel et al., 2009). Therefore, PS-NH<sub>2</sub> can easily pass the cell membrane and trigger toxicity, leading to physiological disruption (e.g. embryotoxicity, larvae malformations, moulting and reduced swimming) and mortality (reviewed in Corsi et al., 2020; Venâncio et al., 2019).

Our recent *in vitro* study on Antarctic sea urchin (*Sterechinus neumayeri*) immune cells showed that, PS NPs (at 1 and 5 µg/mL, after 6 and 24 h exposure) were able to cross the cell membrane in sea urchin coelomocytes and to cause immunomodulation (i.e. decrease in phagocytosis and modulation of stress-related genes) under Antarctic-like exposure conditions (Bergami et al., 2019).

Being well adapted to extreme but stable environmental conditions, with unique phenotypic traits, Antarctic species are considered more vulnerable to environmental perturbations and pollutants, compared to species from different latitudes (Meyer et al., 2015; Zane and Patarnello, 2000). Thus, nanoplastics might pose a threat to Antarctic marine biota and more efforts should be posed in identifying potential biological targets among Antarctic keystone species, in which toxicodynamics should be investigated for proper environmental risk assessment.

Within Antarctic pelagic ecosystems, krill certainly plays a pivotal role as middle trophic level, ensuring high-energy transfer between primary producers and many higher predators, specialized to feed on this species (Atkinson et al., 2012; Trathan and Hill, 2016). Krill has an circumpolar distribution in the Southern Ocean, but almost 70% of its stock is concentrated in the Atlantic sector (0–90° W), corresponding to areas of high primary production and wide extensions of the Antarctic Circumpolar Current (ACC) (Atkinson et al., 2008). In this region, krill is also a fundamental conduit of biogeochemical processes, including nutrient recycling, benthic-pelagic coupling, and carbon (C) sequestration (Cavan et al., 2019; Lehette et al., 2012). Krill FPs, which sink at speeds of hundreds of metres per day, provide pulses of C that can dominate the particulate organic carbon (POC) flux through the mesopelagic (Accornero et al., 2003; Belcher et al., 2019). Krill generally amasses in swarms, which can reach up to 100 km<sup>2</sup> and 2 million tonnes (Tarling and Fielding, 2016), releasing considerable quantities of large dense FPs, which often over-saturate the remineralising community with high C export efficiencies (Belcher et al., 2019).

As with many endemic Antarctic invertebrates, this species is stenothermal and highly sensitive to environmental perturbations throughout its life cycle (Atkinson et al., 2008). Long-term monitoring surveys over the last 40 years (see KRILLBASE, Atkinson et al., 2017) have demonstrated a significant decline in krill densities since 1970s, related to the increasing anthropogenic pressure (Atkinson et al., 2004) and climate change (Atkinson et al., 2019). In this context, the presence of nanoplastics may constitute an additional stressor able to disrupt key ecological processes and ecosystem functioning (Yang et al., 2020), such as a significant shift in the marine microbial community (Urbanek et al., 2017).

Here we explore the impact of two surface charged PS NPs on krill juveniles by acute exposure (48 h) under controlled conditions. We assess the influence of these model nanoplastics on krill physiology (such as swimming and moulting) and discuss the potential effects on fitness as well as changes in microbiome of the surrounding exposure media (SW). Further, we investigate the ingestion/egestion processes and, through the changes in krill FP characteristics upon PS NP exposure, we provide new insight on the potential impact of nanoplastic pollution on the biological mechanisms regulating the export of C in the Southern Ocean. Finally, we characterise the microbial communities in SW associated to PS NP exposure.

## 2. Materials and methods

### 2.1. PS NP behaviour in SW from the Scotia sea

PS NP suspensions were purchased from Bangs Laboratories Inc. A nominal size of 62 and 60 nm was reported for unlabelled and labelled PS-COOH, respectively, and 50 nm for PS-NH<sub>2</sub>. Details about NP stocks and additives are reported in the Supporting Information (SI) and Table S1. PS NP stocks were bath sonicated (CEIA CP316 digit, maximum power 600 W, nominal frequency 40 kHz, amplitude 90%) for 2 min, diluted in milli-Q water (mQW). On board RRS James Clark Ross (JCR, UK) vessel, SW (sea surface T 2.5 °C, salinity 34‰, pH 7.9) was collected from krill sampling sites in the NW region of South Georgia Island (Fig. S1A, Table S2) and stored upon filtration at 0.2 µm. PS NP suspensions were freshly prepared in SW and quickly vortexed prior to use. Dynamic Light Scattering (DLS) was used for physical-chemical characterization of 50 µg/mL NP suspensions in mQW (as reference for NP stability, optimal dispersion and absence of microbial growth) and SW (as exposure medium). Measurements of Z-average (nm) and polydispersity index (PDI, dimensionless) were carried out at different time-points (0, 24, 48 h) at 2 °C, while ζ-potential (mV) was determined by electrophoretic mobility at 4 °C.

### 2.2. Krill sampling and short-term exposure study

Antarctic krill juveniles (*E. superba*) were collected by rectangular midwater trawl (RMT-8) and motion-compensated bongo net in December 2016 in the Southern Ocean sector of the Scotia Sea, near South Georgia Island (UK territory) (Fig. S1A), which represents the northernmost limit of krill stock south ACC (Atkinson et al., 2008).

Soon after sampling, krill juveniles were moved to the cold room (at 2–4 °C) in buckets filled with 0.20 µm filtered SW and maintained in the shade to avoid animal stress. After 12 h, krill juveniles of similar size (30.8 ± 5.2 mm, details in Table S2) displaying an active swimming behaviour were selected for short-term *in vivo* exposure study (48 h). Their age can be estimated between 1 and 1.5 years, assuming an average growth rate of 0.06 mm/d<sup>-1</sup> for Antarctic krill, based on Tarling and Fielding (2016).

Experiments were carried out in the dark, under static conditions at constant temperature of +2 °C in 1L jars containing 0.20 µm filtered SW. Control (only SW) and experimental groups (2.5 µg/mL unlabelled PS-COOH and 2.5 µg/mL unlabelled PS-NH<sub>2</sub>), each containing 3 to 5 organisms (as reported in Table S2), were run in triplicate (Fig. S1B). In each experiment, unlabelled PS NPs were used and an additional experimental group with fluorescently labelled PS-COOH (2.5 µg/mL) was included to investigate PS NP toxicodynamics in krill (Fig. S1B). Animals were not fed during the experiment, which was repeated three times by using krill juveniles collected from 3 different locations (Fig. S1, Table S2). For more details regarding the experimental design, see SI.

Due to the constraints in laboratory setting on board the JCR, it was not possible to expose krill individuals to a concentration gradient. The tested concentration of 2.5 µg/mL was chosen to investigate the sub-lethal effects of nanoplastics on Antarctic krill, based on acute toxicity

thresholds available for PS NPs on other marine zooplankton (Bergami et al., 2017; Manfra et al., 2017). The tested concentration corresponded to about  $2.09 \cdot 10^{10}$  NPs/mL and  $3.64 \cdot 10^{10}$  NPs/mL for 62 nm PS-COOH and 50 nm PS-NH<sub>2</sub>, respectively (equation from “Bangs Laboratories Inc. TechNote 206”). Low residues of stabilisers were present in unlabelled PS-COOH working suspensions, corresponding to 0.025 µg/mL of sodium dodecyl sulfate (SDS) and 0.012 µg/mL of sodium azide (NaN<sub>3</sub>). Their potential role in PS NP toxicodynamics was not evaluated in this study and was considered negligible under the experimental conditions, based on available literature, as reported in the SI (Table S1).

Mortality and moulting were monitored every 24 h. A qualitative observation of krill swimming behaviour, based on the typical individual escape responses of krill to disturbances (O’Brien, 1987), was performed. Studies about krill movements have mostly been conducted using specific laboratory settings, with *ad hoc* large aquaria to track both individual movement and schooling behaviour (Kawaguchi et al., 2010), or through *in situ* observations (Kane et al., 2018). Here, quantitative measurements were not carried out due to constraints in laboratory settings and movements of the vessel at sea.

At the end of each experiment, replicates were merged and 5 specimens per experimental group were stored in RNA Later (Sigma, UK) at  $-80$  °C for gene expression analysis, and 3 specimens per experimental group were fixed in ethanol for microscopy observation. Total length (TL) of individuals was measured ( $n$  krill  $\geq 9$ ) from the anterior margin eye to the telson, excluding the terminal spine according to Everson (2000). Moults (Fig. S2), dead individuals and FPs produced during the incubations were collected at the end of the exposure (48 h) and preserved in ethanol. Furthermore, a pool of FPs excreted from krill juveniles soon after the sampling (Control 0 h) was collected and preserved in ethanol, adopted as environmental reference (i.e. FPs naturally full of NOM) for sinking rate experiments (see Section 2.4.2).

At the end of the experiments, SW corresponding to the sampling sites of krill and SW from each experimental group (Control, PS-COOH, PS-NH<sub>2</sub>) was filtered at 0.22 µm and filters (in duplicate) stored at  $+4$  °C and  $-20$  °C for the analyses on microbial communities, respectively.

### 2.3. Gene expression analysis

Selected genes involved in krill metabolism and moulting were investigated by quantitative reverse transcriptase-polymerase chain reaction (q-RT-PCR), as follows: *fatty acid binding protein (fab)*, *trypsin (try)*, *cuticle protein CB6 (cb6)* and *cuticle 9 (cut9)*. These genes were chosen based on current knowledge of *E. superba* responses to a variety of stressors under laboratory conditions (Seear et al., 2009, 2010) and based on our previous findings on brine shrimp (*Artemia franciscana*) upon exposure to PS NPs (Bergami et al., 2017). *Cb6* is physiologically regulated after apolysis to allow the formation of a new cuticle (Kuballa et al., 2007; Seear et al., 2009). *Glyceraldehyde 3-phosphate dehydrogenase (gapdh)*, *triophosphate isomerase (TPI)* and *phosphoenolpyruvate carboxykinase (pep-ck)* were used as housekeeping genes. Primer sequences are listed in Table S3. RNA extraction, cDNA transcription and q-RT-PCR analysis were performed according to (Vannuccini et al., 2016) and reported in the SI.

### 2.4. PS NP biodistribution and impact on FPs

#### 2.4.1. PS NP biodistribution in FPs

Biodistribution of yellow-green fluorescently labelled PS-COOH (Dragon Green fluorophore, ex/em 480/520) in krill FPs was determined under optical fluorescence microscopy (Olympus BX51) equipped with a Canon EOS 70D camera. FPs from control and fluorescently labelled PS-COOH exposure groups were preserved in ethanol and washed twice in mQW prior imaging in order to remove PS-COOH aggregates from FP surface.

#### 2.4.2. PS NP impact on FP quality

A qualitative observation of krill FP structure was assessed in terms of state of peritrophic membrane and FP surface structure. FPs (from control, PS-COOH and PS-NH<sub>2</sub> groups) were collected at the end of the exposure (48 h) and preserved in ethanol. For the analysis, FPs were washed in mQW, mounted onto stubs using C tape and imaged using a variable pressure scanning electron microscope (VPSEM, Hitachi TM3000). The variable pressure mode allowed the examination of non-conductive samples in their natural state without the need of conventional sample preparation. A total of 30 FPs was imaged ( $n = 10$  for each treatment).

#### 2.4.3. PS NP impact on FP density and sinking rate

In order to determine the effect of nanoplastics on krill FP properties, krill FPs from different groups (Control 0 h, Control 48 h, PS-COOH, PS-NH<sub>2</sub>) were considered. FPs from Control 0 h derived from freshly-caught krill, likely to contain more NOM, reflecting *in situ* feeding activity of krill juveniles in the area near South Georgia Island (as “full” FPs). FPs from Control 48 h were produced by krill juveniles maintained in SW only during the experiments, thus reflecting a short-term starvation of the individuals with no access to food (“empty-like” FPs). FPs from PS-COOH and PS-NH<sub>2</sub> were produced by krill juveniles exposed to 2.5 µg/mL of unlabelled PS NPs for 48 h (see Section 2.2).

All FPs displaying a similar size and shape (cylindrical) ( $n \geq 13$  for each experimental group) were extensively washed in mQW and imaged under a light microscope (Olympus SZX16). Their length (L, mm) and diameter (D, mm) were measured using ImageJ software (Fig. S3). FP volume (V, expressed in µm<sup>3</sup>) was thus obtained as an approximation of a cylinder volume (Fowler and Small, 1972; González, 1992).

Potential sinking rate (m/day) was determined from FP settling velocity ( $\omega_s$ , cm/s), measured under controlled laboratory conditions in a cold room at 8 °C, as described below. For this purpose, each FP was added to 1 L graduated cylinder with 0.20 µm filtered SW (salinity 34‰, pH 8). Each FP was placed at 100 mL under the SW surface to avoid surface tension and allowed to sink for 100 mL (i.e. 68 mm) to attain constant velocity. FP sinking was timed over 200–300 mL, corresponding to 68–102 mm distance between horizontal graduations of the cylinder scale.

FP density ( $\rho_s$ , g/cm<sup>3</sup>) was thus obtained from Stoke’s equation modified for cylindrical particles (Komar et al., 1981), using calculated V and  $\omega_s$ . The sinking behaviour depends on the Reynolds number ( $Re$ , dimensionless), related to FP intrinsic properties (size and settling velocity) and SW parameters. SW density ( $\rho$ ) and viscosity ( $\mu$ ) values at 8 °C were referred to ITTC (2011), corresponding to 1.027 g/cm<sup>3</sup> and 0.0148 g/cm·s, respectively.

The application of the Stoke’s equation is valid for  $(\rho \omega_s L) / \mu < 2$  and  $Re < 0.5$  (Komar et al., 1981). For Euphausiids, variable  $Re$  between 0.22 and 4.1 has been reported (Fowler and Small, 1972), depending on FP size and NOM content. In our study, average  $(\rho \omega_s L) / \mu$  was  $< 2$  and  $Re$  ranged between  $0.030 \pm 0.01$  and  $0.15 \pm 0.06$  for Control 48 h and Control 0 h (i.e. FPs from krill soon after the sampling), respectively, fulfilling the conditions for the application of the Stoke’s equation.

### 2.5. Changes in SW microbiome during PS NP exposure

#### 2.5.1. Bacterial counting (DAPI)

Filters obtained from SW samples in sampling sites and corresponding to experimental groups (SW, Control, PS-COOH and PS-NH<sub>2</sub>) were incubated (15’) with 1 mg/mL Tween 80 in an ultrasonic cleaner bath (Branson 1200 Ultrasonic Cleaner, Branson, USA) to ensure bacterial dispersion (Cappello et al., 2015). After centrifugation (8 min, 8000g) the water containing Tween 80 was collected and the samples processed according to Cappello et al. (2015). DAPI counting was performed on cells fixed with 2% formaldehyde.

### 2.5.2. Total RNA extraction, q-RT-PCR and 16S rRNA clone libraries

Total RNA was extracted from samples of the same group (SW, Control, PS-COOH, PS-NH<sub>2</sub>) in each experiment using the FastRNA® Pro soil direct kit (MP Biomedicals™) (Roussel et al., 2009) and pooled. cDNA was obtained via reverse transcription using First-Strand cDNA Synthesis SuperScript™ II Reverse Transcriptase (Life Technologies) following the manufacturer's protocol. 16S rRNA genes were amplified from total cDNA using the universal primers (530F [5'-GTGCCAGCMG CCGCGG-3'] and 1492R [5'-TACGGYTACCTGTTCAGACT-3']) (Genovese et al., 2014; Lane, 1991). Purified 16S rDNA amplicons were further cloned into the pGEM T-easy Vector II (Promega), transformed into E. Coli DH10β cells and subsequently amplified with primers, specific for the pGEM T-easy vector (M13F (5'-TGTAACAACGAC GGCCAGT-3') and M13R (5'-TCACACAGGAAACAGCTATGAC-3')). Positive products were purified and sequenced by Macrogen (Amsterdam, The Netherlands). Sequences were checked for possible chimeric origin using Pintail 1.1 software (Ashelford et al., 2005). For the 16S rRNA gene sequences, initial alignment of amplified sequences and close relatives identified with BLAST (Altschul et al., 1997).

### 2.6. Statistical analysis

All statistical analyses were performed using Graphpad Prism 5. Normality was verified using Shapiro-Wilk test and homogeneity of variances by Bartlett's test. Since some experimental groups were not conformed to normality assumptions, data were further analysed by non-parametric Kruskal-Wallis test with Dunn's *post hoc* test. Significant differences respect to the control group were considered when  $p < 0.05$ .

## 3. Results

### 3.1. PS NP behaviour in Antarctic SW

Results of NP characterization are reported in Table 1. Intensity-based distributions of PS NPs at different time-points in mQW and SW are shown in Fig. 1. DLS analysis confirmed an optimal dispersion of PS NPs in mQW at 2 °C and stability over a 48 h period, confirming the absence of microbial contamination in NP stocks. On the opposite, large agglomerates ( $861.8 \pm 149$  nm) were observed for anionic PS-COOH in SW and a narrow size distribution for cationic PS-NH<sub>2</sub> ( $51.1 \pm 1.72$  nm), which kept their nominal size, as confirmed by PDI values. Measurements of  $\zeta$ -potential confirmed negative charge of PS-COOH ( $-19.3 \pm 1.62$  mV) and the positive charge of PS-NH<sub>2</sub> ( $+16.4 \pm 3.47$  mV) in SW. The distinct behaviour of PS NPs was also verified in SW from two distant sampling sites in the Scotia Sea (Fig. S4) and during exposure time (Fig. 1), with a slight increase in the agglomeration of PS-COOH in SW (Z-average of  $1043 \pm 121$  nm at 48 h), opposed to the monodisperse PS-NH<sub>2</sub> during krill experiments.

**Table 1**

Behaviour of PS NPs suspensions in mQW and SW (50 µg/mL) at different time-points. Z-average (nm) and PDI were measured at 2 °C. Values are presented as mean  $\pm$  SD of 3 measurements.

Medium	Time (h)	62 nm PS-COOH		50 nm PS-NH <sub>2</sub>	
		Z-Average (nm)	PDI	Z-Average (nm)	PDI
mQW	0	$61.26 \pm 3.4$	$0.067 \pm 0.032$	$46.57 \pm 3.06$	$0.126 \pm 0.01$
	24	$61.12 \pm 2.54$	$0.148 \pm 0.023$	$46.60 \pm 6.76$	$0.208 \pm 0.004$
	48	$55.49 \pm 5.62$	$0.101 \pm 0.036$	$38.99 \pm 4.68$	$0.209 \pm 0.017$
SW	0	$861.8 \pm 149$	$0.216 \pm 0.06$	$51.1 \pm 1.72$	$0.154 \pm 0.01$
	24	$1320 \pm 163.6$	$0.207 \pm 0.012$	$52.61 \pm 6.10$	$0.192 \pm 0.008$
	48	$1043 \pm 121.2$	$0.220 \pm 0.018$	$56.83 \pm 3.13$	$0.216 \pm 0.012$

### 3.2. Impact on krill juveniles

No dead organisms were found upon exposure to 2.5 µg/mL PS NPs in the three experiments. After 48 h, krill juveniles from Control and PS-COOH groups exhibited an active swimming behaviour and a typical escape response to disturbances, as described by O'Brien (1987). When tweezers were inserted in the jars, all the organisms displayed the typical tail-flip reaction, with an increase in the pleopod-swimming velocity, to avoid the stationary object in their trajectories (O'Brien, 1987). Several attempts were thus necessary to collect the organisms from Control and PS-COOH groups. On the contrary, PS-NH<sub>2</sub> clearly modulated thigmotaxis in Antarctic krill. Exposed individuals were characterised by a reduced swimming behaviour, with > 90% of the organisms not actively responding to disturbances and collected by tweezers at the first attempt, within 10 s. An increase in the number of exuviae was also found upon exposure to both PS NPs, while they were absent in the control group. In particular, the moulting reached  $12.59 \pm 1.28\%$  in krill juveniles exposed to cationic PS-NH<sub>2</sub>, while it was negligible, as  $2.22 \pm 3.85\%$ , for those exposed to anionic PS-COOH.

In order to disclose the molecular basis behind the observed sub-lethal effects of PS NPs at the concentration tested (2.5 µg/mL), the expression of genes associated to metabolism and moulting (*fab trypsin*, *cut9*, *cb6*) was investigated through q-RT-PCR analysis and results are reported in Fig. 2.

No clear modulation of *fab* and *try* genes ( $p > 0.05$ ) was observed upon exposure to PS NPs while both PS NPs were able to up-regulate *cut9* gene and PS-NH<sub>2</sub> further modulated *cb6* gene in comparison with to the control group, although these differences were not significant ( $p > 0.05$ ).

### 3.3. Biodistribution and impact on FPs

#### 3.3.1. Biodistribution of PS NPs

The fluorescent signal from fluorescently labelled PS-COOH NPs was recorded in FPs of krill juveniles upon exposure (2.5 mg/L) (Fig. 3). VPSEM micrographs (Fig. 4) showed an alteration in the structure of FPs following exposure to both PS NPs. In particular, 65% of the FPs were characterized by a smooth coated surface, compared to the rough surface of those collected from Control group at 48 h (SW only).

#### 3.3.2. PS NP impact on FP volume, density and sinking rate

Both PS NPs were found to alter the properties of krill FPs, regardless of their surface charge (Fig. 5). FPs from the PS NP-exposed groups were characterized by an average V of  $8.35 \pm 4.22 \cdot 10^6 \mu\text{m}^3$  and  $7.33 \pm 4.76 \cdot 10^6 \mu\text{m}^3$  for PS-COOH and PS-NH<sub>2</sub>, respectively, which was significantly higher ( $p < 0.001$ ) than the average V of more empty-like FPs of Control 48 h ( $4.32 \pm 4.23 \cdot 10^6 \mu\text{m}^3$ ), but comparable to the average V of full FPs of Control 0 h ( $10.27 \pm 4.28 \cdot 10^6 \mu\text{m}^3$ ) (Fig. 5A).

FPs of krill juveniles exposed to PS NPs showed average sinking rates of  $58.40 \pm 23.56$  m/d and  $51.23 \pm 28.60$  m/d for PS-COOH

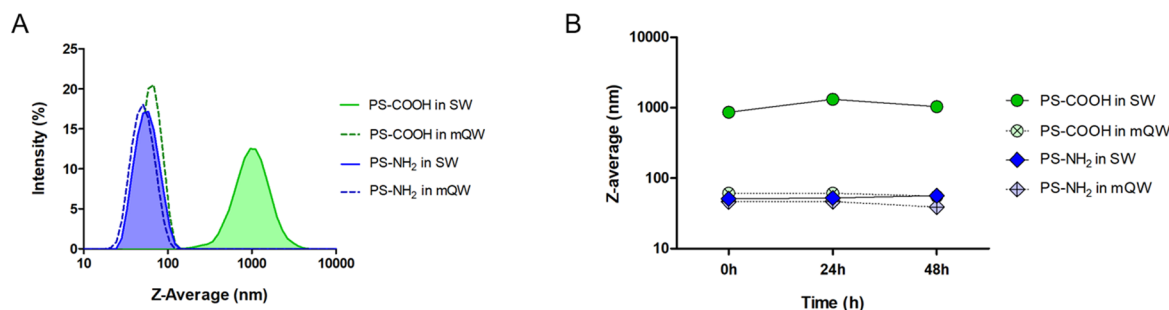


**Fig. 1.** DLS analysis of PS-COOH (green) and PS-NH<sub>2</sub> (blue) suspensions at 50 µg/mL in SW and mQW. (A) Intensity-weighted size distributions and (B) Z-average (nm) at time-points (0, 24, 48 h) in mQW (dotted line) and SW used for krill experiments (area filled). Logarithmic scale is reported for X-axis (A) and Y-axis (B), starting at 10 nm, both showing Z-Average values (nm). The graphs are the average of 3 independent measurements, edited using Graph Pad Prism 5. (For interpretation of the references to colour in this figure legend, the reader is referred to the web version of this article.)

and PS-NH<sub>2</sub>, respectively, which were comparable to the sinking rate of empty-like FPs of Control 48 h (58.02 ± 21.28 m/d), but significantly lower (p < 0.0001) than the sinking rate of FPs of Control 0 h (average of 168.80 ± 74.58 m/d), naturally containing dense organic material (e.g. microalgae cells, NOM), as shown in Fig. 5B.

At last, FPs of PS NP-exposed groups had an average ρ<sub>s</sub> of 1.09 ± 0.02 g/cm<sup>3</sup> and 1.09 ± 0.03 g/cm<sup>3</sup>, similar for PS-COOH and PS-NH<sub>2</sub> but significantly lower (p < 0.0001) than Control 0 h (ρ<sub>s</sub> of 1.17 ± 0.07 g/cm<sup>3</sup>) and also significantly lower (p < 0.05) than Control 48 h (ρ<sub>s</sub> of 1.14 ± 0.04 g/cm<sup>3</sup>) (Fig. 5C).

### 3.4. Change in microbial community

In this study, a first attempt was made to characterize the microbiome associated to PS NP exposure in SW at the end of 48 h incubation. Results from DAPI counting showed a similar number of bacteria in all the experimental groups. The relative abundance of each bacteria

phylum is reported in Fig. 6. A dominance of Proteobacteria (mainly *Psychrobacter*, *Halomonas*, *Pseudomonas* and *Pseudoalteromonas*) was observed in the Control, in contrast to a higher microbial diversity in the groups containing PS NPs in which also Bacteroides, Firmicutes and other unclassified bacteria were found. In the PS NP groups, the microbial composition was more similar to SW from environmental samples used as reference.

### 4. Discussion

Although the recent evidence of macro- and microplastics in waters, sediments and biota around Antarctica (Bessa et al., 2019; Lacerda et al., 2019; Reed et al., 2018; Suaria et al., 2020), the occurrence of nanoplastics in the Southern Ocean remains unexplored. Antarctic krill has been recently found able to fragment ingested microplastics (Dawson et al., 2018a), potentially contributing to the release of large quantities of nanoplastics, which impact on Antarctic marine organisms

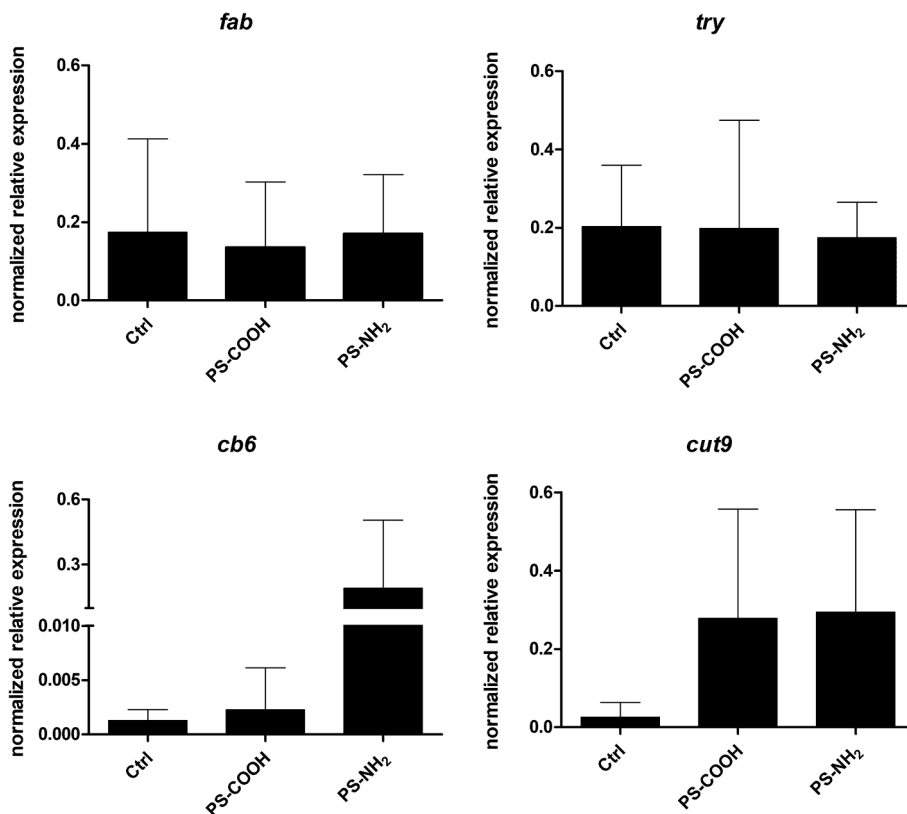


**Fig. 2.** Normalized relative expression (mean ± SD) of selected genes (*fab*, *try*, *cb6*, *cut9*) involved in metabolism and moulting of krill juveniles after 48 h of exposure to PS NPs at 2.5 µg/mL.

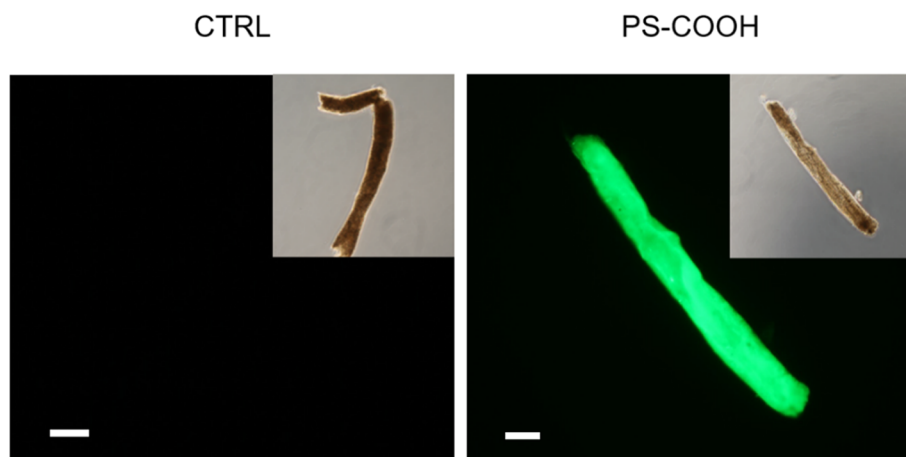


Fig. 3. FPs from krill juveniles of the Control (only SW) and yellow-green fluorescently labelled PS-COOH (2.5  $\mu\text{g}/\text{mL}$ ) groups collected after 48 h of incubation, observed under optical fluorescent microscopy. Scale bar: 100  $\mu\text{m}$ . (For interpretation of the references to colour in this figure legend, the reader is referred to the web version of this article.)

is still overlooked. In the present study, we have characterised the behaviour of surface charged PS NPs, as model nanoplastics, in Antarctic SW media and investigated their toxicodynamics and acute toxicity on Antarctic krill juveniles.

#### 4.1. NP behaviour in Antarctic SW

Data from DLS confirmed the stability of both anionic and cationic PS NPs in mQW over time, in agreement with our previous findings at different temperatures (Bergami et al., 2019; Bergami et al., 2016; Grassi et al., 2019). Anionic PS-COOH suspensions in SW from South Georgia Island were characterised by a pronounced agglomeration at 2  $^{\circ}\text{C}$ . This result differs from previous data in SW from King George Island (Maritime Antarctica), in which PS-COOH were present as nanoscale agglomerates (< 200 nm) soon after dispersion, although they also reached a larger size after 24 h, in agreement with the present study (Bergami et al., 2019). On the contrary, cationic PS-NH<sub>2</sub> exhibited a good dispersion in SW from both Antarctic locations and over different time-points, in agreement with other observations in SW from the Mediterranean Sea (Della Torre et al., 2014; Bergami et al., 2016).

Polar marine ecosystems, due to their unique characteristics, might be more vulnerable to anthropogenic stressors, including plastic pollution (Waller et al., 2017). Our findings suggest that the behaviour of model nanoplastics, such as PS NPs, mainly depends on NP surface charge and SW characteristics. For PS-COOH NPs, differences in NP behaviour observed in Antarctic marine waters and in the Mediterranean Sea (Della Torre et al., 2014; Bergami et al., 2016) may be related to the lower salinity and sea surface temperature of the SW collected in the Scotia Sea (salinity 34‰, sea surface T < 4  $^{\circ}\text{C}$ ) in the present study. Additional SW parameters, related for example to ionic species, NOM composition and other inorganic and organic compounds present in SW may also play a role in driving NP behaviour and fate (Cai et al., 2018; Zhang et al., 2019). This underlines the need for a case-by-case

characterization analysis of PS NPs, and in general of anthropogenic NPs, in aquatic matrices for the correct interpretation of exposure conditions, bioavailability and toxicity assessment (Vijver et al., 2018).

#### 4.2. Consequences on krill fitness

No acute toxicity was found in krill juveniles after short-term exposure to PS NPs (2.5  $\mu\text{g}/\text{mL}$ ), in agreement with Dawson et al. (2018b), in which no mortality was observed in krill upon exposure to PE MPs. Nevertheless, sub-lethal effects, such as the change in krill swimming and moulting, were observed in response to cationic PS NPs. This is in line with our previous studies on marine zooplankton in which toxicity was mostly induced by PS-NH<sub>2</sub>, whereas PS-COOH did not cause significant effects at the organism and population level (reviewed in Corsi et al., 2020). The lack of toxicity of anionic PS NPs has mainly been associated to two features: the electrostatic repulsion with cell membranes (Bhattacharya et al., 2010) and the large NP agglomeration in SW, with consequent loss of typical nanoscale properties and reactivity (Bergami et al., 2017).

Regarding PS-NH<sub>2</sub>-related effects, the higher number of moults suggest the alteration of hormone-controlled processes regulating growth and moulting, in agreement with our previous findings with *A. franciscana* larvae (Bergami et al., 2017, 2016; Varó et al., 2019). In Antarctic krill, moulting implies prominent physiological changes and high-energy costs (Seear et al., 2010) but has also been reported as an instantaneous and synchronous process triggered by external stimuli (Hamner et al., 1983). Through moulting, euphausiids can shrink or grow, adapting to the environmental conditions or removing pathogens and endoparasites (Ikeda and Dixon, 1982; Tarling and Cuzin-Roudy, 2008), since krill moults can include parts of their stomach and hind-guts (Ikeda et al., 1984). Therefore, such complex physiological process can be used as a defence mechanism towards PS-NH<sub>2</sub>, as previously hypothesised for *A. franciscana* larvae (Bergami et al., 2016).

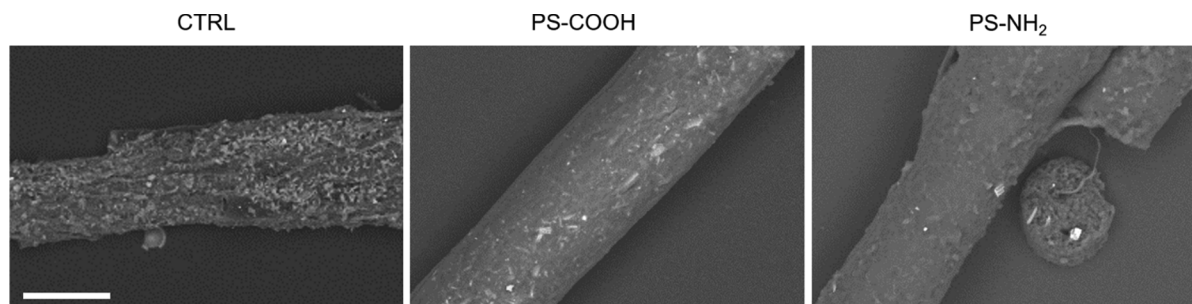


Fig. 4. Representative VPSEM images showing FPs from krill juveniles of the Control (only SW), PS-COOH and PS-NH<sub>2</sub> groups after 48 h of incubation. Scale bar: 50  $\mu\text{m}$ .

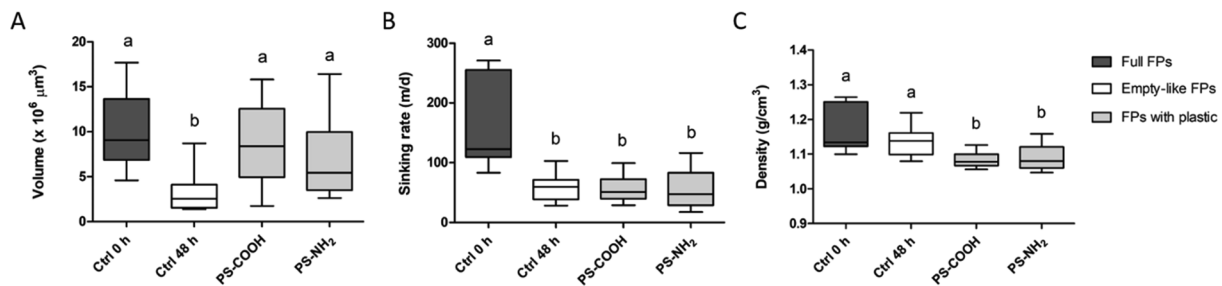


Fig. 5. Box-and-Whisker plots showing krill FP cylindrical volume ( $V$ ,  $\mu\text{m}^3$ , calculated) (A), and sinking rate (m/d, measured) (B) and density ( $\rho_s$ ,  $\text{g}/\text{cm}^3$ , estimated) (C), as mean  $\pm$  SD. FPs ( $n \geq 13$ ) were collected soon after the sampling as reference for full FPs (Ctrl 0 h, in dark grey), after 48 h incubation in SW as reference for more empty-like FPs (Ctrl 48 h, in white) and after 48 h exposure to  $2.5 \mu\text{g}/\text{mL}$  PS-COOH and PS-NH<sub>2</sub> as FPs containing nanoplastic (in light grey). Letters indicate significant differences between the groups (Kruskall-Wallis test, Dunn's *post hoc* test,  $p < 0.05$ ).

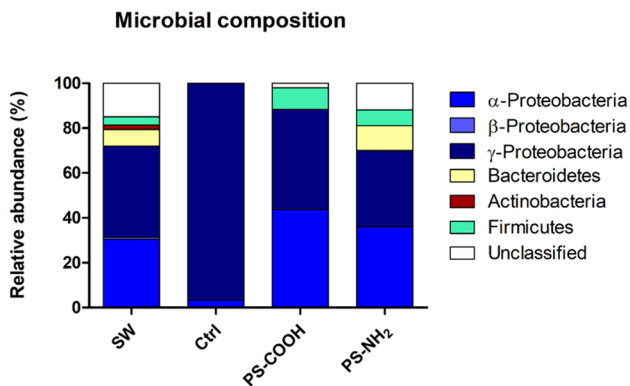


Fig. 6. Relative abundance (%) of different bacteria phyla associated with the experimental groups (Control, exposed to PS-COOH, exposed to PS-NH<sub>2</sub>) and SW from the sampling sites, reported as mean values of 3 experiments.

In this study, change in swimming behaviour has also been observed in krill exposed to PS-NH<sub>2</sub>, with respect to Control and PS-COOH groups. Krill individuals are known as active swimmers, reaching up to 600 mm/s with quick reaction times and high endurance (Kils, 1981), typical of their schooling behaviour (Kawaguchi et al., 2010; O'Brien, 1987). In response to disturbances, three levels of escape behaviour have been described in euphausiids, which, under normal conditions, exhibit typical quick tail-flip reaction and increase in pleopod-swimming velocity (O'Brien, 1987). The lack of a clear avoidance reaction upon 48 h exposure to PS-NH<sub>2</sub> has been observed, suggesting that cationic nanoplastics may impair krill ability to escape predators, which in turn would affect its survival.

Similar swimming alterations have already been observed in brine shrimp larvae exposed to the same NPs, which were found in the digestive tract of the organisms, but also externally on the body and appendages, clearly hampering larvae motility (Bergami et al., 2016). Such internalization of PS-NH<sub>2</sub> and surface adsorption at 48 h were predictive of severe physiological disruption, toxicity and mortality over prolonged exposure, with an LC<sub>50</sub> of  $0.83 \mu\text{g}/\text{mL}$  calculated at 14 days (Bergami et al., 2017; Varó et al., 2019).

In krill juveniles, at the NP concentration tested, PS-NH<sub>2</sub> were not found adsorbed onto their body, however results from VPSEM and sinking rate measurements indicate that cationic NPs were ingested and egested in the exposed organisms. As a consequence, NPs may have been in contact with krill stomach and digestive gland as nanoscale objects, internalised by epithelial cells and caused toxicity. In *A. franciscana* larvae, a significant decrease in cholinesterase and carboxylesterase activities was found upon 48 h exposure to PS-NH<sub>2</sub> ( $1 \mu\text{g}/\text{mL}$ ), suggesting neurotoxicity which affects the swimming behaviour as well as disruption of hormone-related processes regulating growth and moulting.

Change in swimming behaviour could also be an indirect effect of

the release of exuviae, since moulting individuals of *E. superba* are normally characterised by a lower swimming capacity, due to the decrease in rigidity of their exoskeleton and thus a lower capacity of impart power to the water (Buchholz, 1989; Johnson and Tarling, 2008). Despite no significant differences in *cb6* and *cut9* gene expression, it cannot be excluded that prolonged exposure times would elucidate the molecular mechanism(s) behind the observed PS-NH<sub>2</sub> sublethal effects on krill juveniles.

Based also on our previous experience with *A. franciscana*, different toxicity mechanisms of PS-NH<sub>2</sub> in krill juveniles can be formulated, following NP biological interaction: i) PS-NH<sub>2</sub> trigger toxicity through oxidative stress and alteration in cholinergic activities, with changes in swimming behaviour and moulting (both direct effects). ii) PS-NH<sub>2</sub> alter signalling cascades that disrupt hormone-regulated processes, such as growth and moulting. As a consequence, a decrease in swimming of moulting individuals is observed as an indirect effect. iii) a combination of the two mechanisms of action occurs.

Our results underline a similar PS-NH<sub>2</sub> toxicodynamic in *A. franciscana* larvae and *E. superba* juveniles with potential repercussions on their physiology and survival over long-term exposure scenarios, which could be the subject of future studies to understand the toxicity mechanisms at the molecular and biomolecular level.

#### 4.3. Potential implication for Southern Ocean C export

In our study, we have indirectly showed the ingestion and egestion of PS NP agglomerates by krill juveniles, through the incorporation of fluorescently labelled PS-COOH in krill FPs, but also through VPSEM and the analysis of FP properties.

FPs normally contain densely packed NOM and undigested components enclosed within the peritrophic membrane produced in the hindgut of krill (Schmidt and Atkinson, 2016). Here we demonstrated that both PS NPs, regardless of their surface charges, significantly altered FP properties by comparison with: (i) full FPs of Control 0 h, derived from well-fed krill soon after collection (comparison plastic vs food); (ii) more empty-like FPs of Control 48 h derived from krill individuals maintained in SW for about 60 h considering the pre-exposure period (comparison plastic vs lack of food). The distinction in the amount of food content between Control 0 h and Control 48 h explains the significant difference in FP V found in these two groups.

With respect to Control 48 h, the significant increase in FP V observed upon exposure to nanoplastics was attributed to krill feeding on PS NPs. At the tested concentration ( $2.5 \mu\text{g}/\text{mL}$  equal to about  $2.09\text{--}3.64 \cdot 10^{10}$  NPs/mL), krill juveniles were exposed to large quantities of suspended particles in the picoplankton (size  $0.2\text{--}2 \mu\text{m}$ , considering small NP agglomerates) and nanoplankton range ( $> 2 \mu\text{m}$ , for large NP agglomerates), which were actively ingested. While swimming, krill can efficiently filter a broad range of prey (Kils, 1981), ranging from nanoplankton up to giant diatoms and large zooplankton, thanks to the filtering surface of its feeding basket with a mesh size of

2–3  $\mu\text{m}$  (Kils, 1983; Schmidt and Atkinson, 2016).

The exceptional feeding behaviour of the Antarctic krill supports our observation of the ingestion of nanoplastic agglomerates and suggest that krill can be exposed to a wide range of plastic particles, from microplastics (Dawson et al., 2018a,b) down to nanoplastics, with an exceptional ecological adaptation to different prey size.

The present study also demonstrates that Antarctic krill is able to feed on nanoplastic agglomerates in the absence of food, reflecting natural environmental conditions characterized by the paucity of food resources, such as during the Antarctic winter. All together, these results strongly suggest a continuous biodistribution of micro- and nanoplastics to polar coprophagous planktonic species, and a potential transfer along marine trophic webs.

The low FP sinking rate of Control 48 h (compared to Control 0 h) was attributed to the low NOM content and smaller  $V$ , while for PS-COOH and PS-NH<sub>2</sub> it was related to the incorporation of low-density PS NPs into the FP matrix. According to the manufacturer, PS NPs are characterised by a density of 1.05–1.06 g/cm<sup>3</sup>, thus being neutrally buoyant in SW (Andrady, 2017). As a consequence, the incorporation of low dense PS NPs into FPs can significantly alter their sinking velocities in the water column compared to FPs containing NOM, algae and/or copepods (Control 0 h), as confirmed by our findings.

At last, FP  $\rho_s$  was obtained based on the other measured parameters, from the Stoke equation (Komar et al., 1981) and shown to strictly depend on FP  $V$  and sinking rate measured. Here, a significant difference between Control 0 h and PS NP groups was found due to the diverse dense material incorporated in the FPs (i.e. microalgae, copepods and/or large diatoms vs plastic agglomerates). With respect to Control 0 h, the lower but comparable FP  $\rho_s$  of Control 48 h was attributed to the low FP diameter and consequently low  $V$  obtained for the latter group (i.e., empty-like FPs of Control 48 h), which influenced the Stoke equation for FP  $\rho_s$  calculation. The difference in FP  $V$  between Control 48 h and PS NP treatments further confirms the absence of artefacts in the experimental design.

In this study, krill juveniles were not fed during the experiments. Feeding the organisms in such limited exposure period would have increased the variability in the system, with unknown effects on the results observed, in particular for the changes in gene expression and in microbial communities, which would have been far more challenging to interpret.

Under natural conditions, nanoplastic ingestion and egestion in the Antarctic krill are likely to occur also in presence of food sources. Dawson et al. (2018a) found micro- and sub-micron PE in the FPs of Antarctic krill adults exposed to a mixed diet of PE MPs and microalgae. In our previous study, we observed a strong adsorption of PS NPs onto the microalgae cells, which were in turn ingested by brine shrimp larvae and incorporated in their FPs (Bergami et al., 2017).

In case of plastic exposure occurring in presence of food, we expect similar FP  $V$  compared to full FPs in the Control group but differences in FP sinking rate and  $\rho_s$ , caused by the incorporation of low-density NPs into the FP matrix. Similar results have been reported in zooplankton, such as copepods and salps, upon exposure to microplastics (Cole et al., 2016; Coppock et al., 2019; Wiczczyk et al., 2019).

To our knowledge, this is the first study showing the impact of nanoplastics on FP properties and sinking rates. The Southern Ocean represents an important part of the global C sink and faeces of zooplankton are major vehicles for C transfer and sequestration to the deep ocean (Accornero et al., 2003; Manno et al., 2015). The crucial role of *E. superba* in biogeochemical cycles has recently been recognised (Cavan et al., 2019), since within the Southern Ocean, the presence of krill swarms can significantly increase the efficiency of the biological C pump by the production of a “rain” of fast sinking FPs, (up to 800 m/day) that overwhelm detrital consumers (Belcher et al., 2017; Cadée et al., 1992; Tarling and Fielding, 2016).

We suggest that the incorporation of NPs could increase FP residence time in the epipelagic zone (from surface to 200 m depth), with

higher susceptibility to remineralization by zooplankton and prokaryotes, which will impact the amount of C exported to the deep ocean (Iversen and Poulsen, 2007; Svendsen et al., 2014, 2012).

#### 4.4. Potential implication for marine microbiome

As a preliminary investigation, we examined the microbial communities in SW following krill exposure to PS NPs and compared them to SW samples from surface waters in same locations of krill sampling. It is worthy to note that PS-NH<sub>2</sub> suspensions did not contain stabilisers, whereas a low amount of SDS (0.025  $\mu\text{g}/\text{mL}$ ) and NaN<sub>3</sub> (0.012  $\mu\text{g}/\text{mL}$ ) was present in unlabelled PS-COOH working suspensions. Based on EC<sub>50</sub> values of these two surfactants available for model marine bacteria *Vibrio fischeri* (Table S1), the potential effect of SDS and NaN<sub>3</sub> residues in PS-COOH suspensions was considered negligible for SW microbiome, however an experimental group containing SW and surfactants only was not included in the analysis. Future studies should disentangle the role of surfactants present in commercially available nanoplastic suspensions (Heinlaan et al., 2020).

Antarctic krill has been shown to largely contribute to the whole marine bacterial assemblages of the Southern Ocean, being responsible for the transport of unique bacterial communities, which can be uncommon in the surrounding SW (Clarke et al., 2019). In agreement with these findings, our study confirmed that distinct bacteria phyla, such as Actinobacteria and Firmicutes, present in SW samples were surprisingly found only in SW from krill exposed to PS NPs, but not in Control groups (unexposed krill in SW). In this latter group, only the most common cultured bacteria associated to Antarctic krill were identified (Gómez-Gutiérrez and Morales-Ávila, 2016).

Microbial communities have been found to significantly differ in SW samples and krill within the same location, as well as in the krill itself, with different relative abundance of bacteria found associated with the digestive tract, moults and faeces (Clarke et al., 2019). According to Clarke et al. (2019), moults can largely contribute to the bacterial communities found in surface waters. The release of moults observed upon PS NP exposure further supports the similarities found in microbial communities with natural SW.

Considering the important role of krill and its FPs in shaping the composition of microbial communities in the Southern Ocean, any change may significantly alter such delicate equilibrium. The life cycle of krill epibionts, pathogens (including bacteria) and endoparasites strictly depends on the moulting events of the host (Gómez-Gutiérrez and Morales-Ávila, 2016). Further studies should elucidate how PS NPs might affect the microbiome of Antarctic krill in order to assess any potential repercussion at the ecosystem level.

## 5. Conclusions

Under future business-as-usual scenario, the production of plastic polymers is estimated to reach up to 265 million metric tonnes per year in 2060 (Lebreton and Andrady, 2019), with an enormous amount of mismanaged plastic waste reaching seas and oceans worldwide. Without concrete efforts against plastic pollution, the continuous ingestion of micro- and nanoplastics in marine zooplankton and incorporation in FPs will likely have an impact on the marine biogeochemical cycle and ecosystem functioning. These considerations are particularly relevant for the Antarctic krill, a keystone species in the Southern Ocean already facing changes in distribution and recruitment in relation to climate change (Atkinson et al., 2019; Hill et al., 2019). This species has recently been found to graze on plastic debris, releasing a high number of nanoscale fragments, which impacts are largely unknown. The present study provides cues about the potential consequences due to the interaction between krill and nanoplastics on the Southern Ocean marine ecosystems and C cycle.



## Credit authorship contribution statement

**E. Bergami:** Conceptualization, Methodology, Data curation, Writing. **C. Manno:** Conceptualization, Methodology, Data curation, Writing. **S. Cappello:** Methodology. **M.L. Vannuccini:** Methodology. **I. Corsi:** Funding acquisition, Conceptualization, Methodology, Data curation, Writing.

## Declaration of Competing Interest

The authors declare that they have no known competing financial interests or personal relationships that could have appeared to influence the work reported in this paper.

## Acknowledgements

This study was performed within Nanopolymers in the Antarctic marine environment and biota project, founded by the Italian National Antarctic Program (PNRA 16.00075), in collaboration with the British Antarctic Survey (BAS, Cambridge, UK). We thank the officers and crew of the RRS “James Clark Ross” and the researchers from BAS Ecosystems team for the support prior and during the JR16003 expedition. DLS analysis was conducted at the Dep. of Biotechnologies, Chemistry and Pharmacy (University of Siena, Italy), with the support of Prof. Atrei and Dr. Uva. FP analysis was partially conducted by EB at BAS facilities within the LLP Erasmus (year 2016–2017).

## Appendix A. Supplementary material

Supplementary data to this article can be found online at <https://doi.org/10.1016/j.envint.2020.105999>.

## References

- Accornero, A., Manno, C., Esposito, F., Gambi, M.C., 2003. The vertical flux of particulate matter in the polynya of Terra Nova Bay. Part II. Biological components. *Antarct. Sci.* 15, 175–188. <https://doi.org/10.1017/S0954102003001214>.
- Altschul, S.F., Madden, T.L., Schäffer, A.A., Zhang, J., Zhang, Z., Miller, W., Lipman, D.J., 1997. Gapped BLAST and PSI-BLAST: a new generation of protein database search programs. *Nucleic Acids Res.* 25, 3389–3402. <https://doi.org/10.1093/nar/25.17.3389>.
- Andrady, A.L., 2017. The plastic in microplastics: a review. *Mar. Pollut. Bull.* 119, 12–22. <https://doi.org/10.1016/j.marpolbul.2017.01.082>.
- Andrady, A.L., 2011. Microplastics in the marine environment. *Mar. Pollut. Bull.* 62, 1596–1605. <https://doi.org/10.1016/j.marpolbul.2011.05.030>.
- Ashelford, K.E., Chuzhanova, N.A., Fry, J.C., Jones, A.J., Weightman, A.J., 2005. Media release • communiqué aux médias • medienmitteilung. *World* 71, 7724–7736. <https://doi.org/10.1128/aem.71.12.7724>.
- Atkinson, A., Hill, S.L., Pakhomov, E.A., Siegel, V., Anadon, R., Chiba, S., Daly, K.L., Downie, R., Fielding, S., Fretwell, P., Gerrish, L., Hosie, G.W., Jessopp, M.J., Kawaguchi, S., Krafft, B.A., Loeb, V., Nishikawa, J., Peat, H.J., Reiss, C.S., Ross, R.M., Quetin, L.B., Schmidt, K., Steinberg, D.K., Subramaniam, R.C., Tarling, G.A., Ward, P., 2017. KRILLBASE: a circumpolar database of Antarctic krill and salp numerical densities, 1926–2016. *Earth Syst. Sci. Data* 9, 193–210. <https://doi.org/10.5194/essd-9-193-2017>.
- Atkinson, A., Hill, S.L., Pakhomov, E.A., Siegel, V., Reiss, C.S., Loeb, V.J., Steinberg, D.K., Schmidt, K., Tarling, G.A., Gerrish, L., Sailley, S.F., 2019. Krill (*Euphausia superba*) distribution contracts southward during rapid regional warming. *Nat. Clim. Chang.* 9, 142–147. <https://doi.org/10.1038/s41558-018-0370-z>.
- Atkinson, A., Siegel, V., Pakhomov, E., Rothery, P., 2004. Long-term decline in krill stock and increase in salps within the Southern Ocean. *Nature* 432, 100–103. <https://doi.org/10.1038/nature02996>.
- Atkinson, A., Siegel, V., Pakhomov, E.A., Rothery, P., Loeb, V., Ross, R.M., Quetin, L.B., Schmidt, K., Fretwell, P., Murphy, E.J., Tarling, G.A., Fleming, A.H., 2008. Oceanic circumpolar habitats of Antarctic krill. *Mar. Ecol. Prog. Ser.* 362, 1–23. <https://doi.org/10.3354/meps07498>.
- Atkinson, A., Ward, P., Hunt, B.P.V., Pakhomov, E.A., Hosie, G.W., et al., 2012. An overview of Southern Ocean zooplankton data: abundance, biomass, feeding and functional relationships. *CCAMLR Sci.* 19, 171–218.
- Bangs Laboratories Inc. TechNote 206. URL: [www.bangslabs.com/sites/default/files/imce/docs/TechNote\\_206\\_Web.pdf](http://www.bangslabs.com/sites/default/files/imce/docs/TechNote_206_Web.pdf).
- Belcher, A., Henson, S.A., Manno, C., Hill, S.L., Atkinson, A., Thorpe, S.E., Fretwell, P., Ireland, L., Tarling, G.A., 2019. Krill faecal pellets drive hidden pulses of particulate organic carbon in the marginal ice zone. *Nat. Commun.* 10. <https://doi.org/10.1038/s41467-019-08847-1>.
- Belcher, A., Manno, G.A.T.C., Ward, A.A.P., 2017. The potential role of Antarctic krill faecal pellets in efficient carbon export at the marginal ice zone of the South Orkney Islands in spring. *Polar Biol.* 40, 2001–2013. <https://doi.org/10.1007/s00300-017-2118-z>.
- Bergami, E., Bocci, E., Vannuccini, M.L., Monopoli, M., Salvati, A., Dawson, K.A., Corsi, I., 2016. Nano-sized polystyrene affects feeding, behavior and physiology of brine shrimp *Artemia franciscana* larvae. *Ectotoxicol. Environ. Saf.* 123, 18–25. <https://doi.org/10.1016/j.ecoenv.2015.09.021>.
- Bergami, E., Krupinski Emerenciano, A., González-Aravena, M., Cárdenas, C.A., Hernández, P., Silva, J.R.M.C., Corsi, I., 2019. Polystyrene nanoparticles affect the innate immune system of the Antarctic sea urchin *Sterechnus neumayeri*. *Polar Biol.* 42, 743–757. <https://doi.org/10.1007/s00300-019-02468-6>.
- Bergami, E., Pugnali, S., Vannuccini, M.L., Manfra, L., Faleri, C., Savorelli, F., Dawson, K.A., Corsi, I., 2017. Long-term toxicity of surface-charged polystyrene nanoparticles to marine planktonic species *Dunaliella tertiolecta* and *Artemia franciscana*. *Aquat. Toxicol.* 189, 159–169. <https://doi.org/10.1016/j.aquatox.2017.06.008>.
- Bessa, F., Ratcliffe, N., Otero, V., Sobral, P., Marques, J.C., Waluda, C.M., Trathan, P.N., Xavier, J.C., 2019. Microplastics in gentoo penguins from the Antarctic region. *Sci. Rep.* 9, 1–7. <https://doi.org/10.1038/s41598-019-50621-2>.
- Bhattacharya, P., Lin, S., Turner, J.P., Ke, P.C., 2010. Physical adsorption of charged plastic nanoparticles affects algal photosynthesis. *J. Phys. Chem. C* 114, 16556–16561. <https://doi.org/10.1021/jp1054759>.
- Blasco, J., Corsi, I. (Eds.), 2019. Ecotoxicology of nanoparticles in aquatic systems. CRC Press, Taylor and Francis Group, LLC. <https://doi.org/10.1201/9781315158761>.
- Buchholz, F., 1989. Moulting cycle and seasonal activities of chitinolytic enzymes in the integument and digestive tract of the Antarctic krill, *Euphausia superba*. *Polar Biol.* 9, 311–317.
- Cadée, G.C., Gonzalez, H., Schnack-Schiel, S.B., 1992. Krill diet affects fecal string setting. *Polar Biol.* 12, 75–80. <https://doi.org/10.1007/BF00239967>.
- Cai, L., Hu, L., Shi, H., Ye, J., Zhang, Y., Kim, H., 2018. Effects of inorganic ions and natural organic matter on the aggregation of nanoparticles. *Chemosphere* 197, 142–151. <https://doi.org/10.1016/j.chemosphere.2018.01.052>.
- Cappello, S., Calogero, R., Santisi, S., Genovese, M., Denaro, R., Genovese, L., Giuliano, L., Mancini, G., Yakimov, M.M., 2015. Bioremediation of oil polluted marine sediments: a bio-engineering treatment. *Int. Microbiol.* 18, 127–134. <https://doi.org/10.2436/20.1501.01.242>.
- Cavan, E.L., Belcher, A., Atkinson, A., Hill, S.L., Kawaguchi, S., McCormack, S., Meyer, B., Nicol, S., Ratnarajah, L., Schmidt, K., Steinberg, D.K., Tarling, G.A., Boyd, P.W., 2019. The importance of Antarctic krill in biogeochemical cycles. *Nat. Commun.* 10, 1–13. <https://doi.org/10.1038/s41467-019-12668-7>.
- Chiba, S., Saito, H., Fletcher, R., Yogi, T., Kayo, M., Miyagi, S., Ogido, M., Fujikura, K., 2018. Human footprint in the abyss: 30 year records of deep-sea plastic debris. *Mar. Policy* 96, 204–212. <https://doi.org/10.1016/j.marpol.2018.03.022>.
- Clarke, L.J., Suter, L., King, R., Bissett, A., Deagle, B.E., 2019. Antarctic krill are reservoirs for distinct southern ocean microbial communities. *Front. Microbiol.* 10, 1–9. <https://doi.org/10.3389/fmicb.2018.03226>.
- Cole, M., Galloway, T.S., 2015. Ingestion of nanoplastics and microplastics by pacific oyster larvae. *Environ. Sci. Technol.* 49 (24), 14625–14632. <https://doi.org/10.1021/acs.est.5b04099>.
- Cole, M., Lindeque, P.K., Fileman, E., Clark, J., Lewis, C., Halsband, C., Galloway, T.S., 2016. Microplastics alter the properties and sinking rates of zooplankton faecal pellets. *Environ. Sci. Technol.* 50, 3239–3246. <https://doi.org/10.1021/acs.est.5b05905>.
- Coppock, R.L., Galloway, T.S., Cole, M., Fileman, E.S., Queirós, A.M., Lindeque, P.K., 2019. Microplastics alter feeding selectivity and faecal density in the copepod, *Calanus helgolandicus*. *Sci. Total Environ.* 687, 780–789. <https://doi.org/10.1016/j.scitotenv.2019.06.009>.
- Corsi, I., Bergami, E., Grassi, G., 2020. Behaviour and bio-interactions of anthropogenic particles in marine environment for a more realistic ecological risk assessment. *Front. Environ. Sci.* 8, 60. <https://doi.org/10.3389/fenvs.2020.00060>.
- Cózar, A., Echevarría, F., González-Gordillo, L.I., Irigoien, X., Úbeda, B., Hernández-León, S., Palma, Á.T., Navarro, S., García-de-Lomas, J., Ruiz, A., Fernández-de-Puelles, M.L., Duarte, C.M., 2014. Plastic debris in the open ocean. *Proc. Natl. Acad. Sci. USA* 111, 10239–10244. <https://doi.org/10.1073/pnas.1314705111>.
- Dawson, A., Kawaguchi, S., King, C.K., Townsend, K.A., King, R., Huston, W.M., Bengtson Nash, S.M., 2018a. Turning microplastics into nanoplastics through digestive fragmentation by Antarctic krill. *Nat. Commun.* 9, 1001. <https://doi.org/10.1038/s41467-018-03465-9>.
- Dawson, A., Huston, W., Kawaguchi, S., King, C., Cropp, R., Wild, S., Eisenmann, P., Townsend, K., Bengtson Nash, S.M., 2018b. Uptake and Depuration Kinetics Influence Microplastic Bioaccumulation and Toxicity in Antarctic Krill (*Euphausia superba*). *Environ. Sci. Technol.* 52, 3195–3201. <https://doi.org/10.1021/acs.est.7b05759>.
- Della Torre, C., Bergami, E., Salvati, A., Faleri, C., Cirino, P., Dawson, K.A., Corsi, I., 2014. Accumulation and embryotoxicity of polystyrene nanoparticles at early stage of development of sea urchin embryos *Paracentrotus lividus*. *Environ. Sci. Technol.* 48. <https://doi.org/10.1021/es502569w>.
- Everson, I., 2000. In: Everson, I. (Ed.), *Krill Biology, Ecology and Fisheries. Fish and aquatic resources series Blackwell Science, Oxford*, pp. 1–372.
- Fowler, S.W., Small, L.F., 1972. Sinking rates of euphausiid fecal pellets. *Limnol. Oceanogr.* 293–296. <https://doi.org/10.4319/lo.1972.17.2.0293>.
- Genovese, M., Crisafi, F., Denaro, R., Cappello, S., Russo, D., Calogero, R., Santisi, S., Catalfamo, M., Modica, A., Smedile, F., Genovese, L., Golysheva, P.N., Giuliano, L., Yakimov, M.M., 2014. Effective bioremediation strategy for rapid in situ cleanup of anoxic marine sediments in mesocosm oil spill simulation. *Front. Microbiol.* 5, 1–14. <https://doi.org/10.3389/fmicb.2014.00162>.

- Gómez-Gutiérrez, J., Morales-Ávila, J.R., 2016. Parasites and diseases. In: Siegel, V. (Ed.), *Biology and Ecology of Antarctic Krill*. Advances in Polar Ecology. Springer, pp. 351–386. [https://doi.org/10.1007/978-3-319-29279-3\\_10](https://doi.org/10.1007/978-3-319-29279-3_10).
- González, H.E., 1992. The distribution and abundance of krill faecal material and oval pellets in the Scotia and Weddell Seas (Antarctica) and their role in particle flux. *Polar Biol.* 12, 81–91. <https://doi.org/10.1007/BF00239968>.
- Grassi, G., Landi, C., Della Torre, C., Bergami, E., Bini, L., Corsi, I., 2019. Proteomic profile of the hard corona of charged polystyrene nanoparticles exposed to sea urchin: *Paracentrotus lividus* coelomic fluid highlights potential drivers of toxicity. *Environ. Sci. Nano* 6, 2937–2947. <https://doi.org/10.1039/c9en00824a>.
- Hamner, W.M., Hamner, P.P., Strand, S.W., Gilmer, R.W., 1983. Behavior of Antarctic krill, *Euphausia superba*: chemoreception, feeding, schooling, and molting. *Science* 220 (4595), 433–435. <https://doi.org/10.1126/science.220.4595.433>.
- Hartmann, N.B., Hüffer, T., Thompson, R.C., Hasselöv, M., Verschoor, A., Daugaard, A.E., Rist, S., Karlsson, T., Brennholt, N., Cole, M., Herrling, M.P., Hess, M.C., Ivleva, N.P., Lusher, A.L., Wagner, M., 2019. Are we speaking the same language? Recommendations for a definition and categorization framework for plastic debris. *Environ. Sci. Technol.* 53, 1039–1047. <https://doi.org/10.1021/acs.est.8b05297>.
- Heinlaan, M., Kasemets, K., Aruoja, V., Blinova, I., Bondarenko, O., Lujkanova, A., Khosrovyan, A., Kurvet, I., Pullerits, M., Sihtmäe, M., Vasiliev, G., Vija, H., Kahru, A., 2020. Hazard evaluation of polystyrene nanoplastic with nine bioassays did not show particle-specific acute toxicity. *Sci. Total Environ.* 707, 136073. <https://doi.org/10.1016/j.scitotenv.2019.136073>.
- Hill, S.L., Atkinson, A., Pakhomov, E.A., Siegel, V., 2019. Evidence for a decline in the population density of Antarctic krill *Euphausia superba*. *J. Crustac. Biol.* 39, 316–322. <https://doi.org/10.1093/jcbiol/ruz004>.
- Ikeda, T., Dixon, P., 1982. Body shrinkage as a possible overwintering mechanism of the Antarctic krill, *Euphausia superba* Dana. *J. Exp. Mar. Biol. Ecol.* 62, 143–151.
- Ikeda, T., Nash, G.V., Thomas, P.G., 1984. An observation of discarded stomach with exoskeleton moult from Antarctic krill *Euphausia superba* Dana. *Polar Biol.* 3, 241–244. <https://doi.org/10.1007/BF00229631>.
- ImageJ software (Version 1.49, Wayne Rasband National Institutes of Health, USA): <https://imagej.nih.gov/ij/>.
- Iversen, M.H., Poulsen, L.K., 2007. Coprophagy, coprophagy, and coprochela in the copepods *Calanus helgolandicus*, *Pseudocalanus elongatus*, and *Oithona similis*. *Mar. Ecol. Prog. Ser.* 350, 79–89. <https://doi.org/10.3354/meps07095>.
- Jamieson, A.J., Brooks, L.S.R., Reid, W.D.K., Piertney, S.B., Narayanaswamy, B.E., Linley, T.D., 2019. Microplastics and synthetic particles ingested by deep-sea amphipods in six of the deepest marine ecosystems on Earth. *R. Soc. Open Sci.* 6, 180667. <https://doi.org/10.1098/rsos.180667>.
- Johnson, M.L., Tarling, G.A., 2008. Influence of individual state on swimming capacity and behaviour of Antarctic krill *Euphausia superba*. *Mar. Ecol. Prog. Ser.* 366, 99–110. <https://doi.org/10.3354/meps07533>.
- Jones-Williams, K., Galloway, T., Cole, M., Stowasser, G., Waluda, C., Manno, C., 2020. Close encounters - microplastic availability to pelagic amphipods in sub-antarctic and antarctic surface waters. *Environ. Int.* 140, 105792. <https://doi.org/10.1016/j.envint.2020.105792>.
- Kane, M.K., Yopak, R., Roman, C., Menden-deuer, S., 2018. Krill motion in the Southern Ocean: quantifying in situ krill movement behaviors and distributions during the late austral autumn and spring. *Limnol. Oceanogr.* 9999, 1–19. <https://doi.org/10.1002/lno.11024>.
- Kawaguchi, S., King, R., Meijers, R., Osborn, J.E., Swadling, K.M., Ritz, D.A., Nicol, S., 2010. An experimental aquarium for observing the schooling behaviour of Antarctic krill (*Euphausia superba*). *Deep Res. II* 57, 683–692. <https://doi.org/10.1016/j.dsr2.2009.10.017>.
- Kils, U., 1983. Swimming and feeding of Antarctic krill, *Euphausia superba* – some outstanding energetics and dynamics – some unique morphological details. *Ber Polarforsch* 4, 130–155.
- Kils, U., 1981. Swimming behaviour, swimming performance and energy balance of Antarctic krill, *Euphausia superba*. *Biomass Sci. Ser.* 3, 1–122.
- Komar, P.D., Morse, A.P., Fowler, S.W., 1981. *Euphausiid Fecal Pellets*. *Limnol. Oceanogr.* 26, 172–180.
- Kooi, M., Van Nes, E.H., Scheffer, M., Koelmans, A.A., 2017. Ups and downs in the ocean: effects of biofouling on vertical transport of microplastics. *Environ. Sci. Technol.* 51, 7963–7971. <https://doi.org/10.1021/acs.est.6b04702>.
- Kuballa, A.V., Merritt, D.J., Elizur, A., 2007. Gene expression profiling of cuticular proteins across the moult cycle of the crab *Portunus pelagicus*. *BMC Biol.* 5, 1–26. <https://doi.org/10.1186/1741-7007-5-45>.
- Lacerda, A.L.d.F., Rodrigues, L. dos S., van Sebille, E., Rodrigues, F.L., Ribeiro, L., Secchi, E.R., Kessler, F., Proietti, M.C., 2019. Plastics in sea surface waters around the Antarctic Peninsula. *Sci. Rep.* 9, 3977. <https://doi.org/10.1038/s41598-019-40311-4>.
- Lane, D.J., 1991. 16S/23S rRNA sequencing. In: Stackebrandt, E., Goodfellow, M. (Eds.), *Nucleic Acid Techniques in Bacterial Systematics*. John Wiley & Sons Ltd, New York, pp. 115–175.
- Le Guen, C., Suaria, G., Sherley, R.B., Ryan, P.G., Aliani, S., Boehme, L., Brierley, A.S., 2020. Microplastic study reveals the presence of natural and synthetic fibres in the diet of King Penguins (*Aptenodytes patagonicus*) foraging from South Georgia. *Environ. Int.* 134, 105303. <https://doi.org/10.1016/j.envint.2019.105303>.
- Lebreton, L., Andrady, A., 2019. Future scenarios of global plastic waste generation and disposal. *Palgrave Commun.* 5, 1–11. <https://doi.org/10.1057/s41599-018-0212-7>.
- Lehette, P., Tovar-Sánchez, A., Duarte, C.M., Hernández-León, S., 2012. Krill excretion and its effect on primary production. *Mar. Ecol. Prog. Ser.* 459, 29–38. <https://doi.org/10.3354/meps09746>.
- Manfra, L., Rotini, A., Bergami, E., Grassi, G., Faleri, C., Corsi, I., 2017. Comparative ecotoxicity of polystyrene nanoparticles in natural seawater and reconstituted seawater using the rotifer *Brachionus plicatilis*. *Ecotoxicol. Environ. Saf.* 145, 557–563. <https://doi.org/10.1016/j.ecoenv.2017.07.068>.
- Manno, C., Stowasser, G., Enderlein, P., Fielding, S., Tarling, G.A., 2015. The contribution of zooplankton faecal pellets to deep-carbon transport in the Scotia Sea (Southern Ocean). *Biogeosciences* 12, 1955–1965. <https://doi.org/10.5194/bg-12-1955-2015>.
- Meyer, B., Martini, P., Biscontin, A., De Pittà, C., Romualdi, C., Teschke, M., Frickenhaus, S., Harms, L., Freier, U., Jarman, S., Kawaguchi, S., 2015. Pyrosequencing and de novo assembly of Antarctic krill (*Euphausia superba*) transcriptome to study the adaptability of krill to climate-induced environmental changes. *Mol. Ecol. Resour.* 15, 1460–1471. <https://doi.org/10.1111/1755-0998.12408>.
- Munari, C., Infantini, V., Scoptoni, M., Rastelli, E., Corinaldesi, C., Mistri, M., 2017. Microplastics in the sediments of Terra Nova Bay (Ross Sea, Antarctica). *Mar. Pollut. Bull.* 122, 161–165. <https://doi.org/10.1016/j.marpolbul.2017.06.039>.
- Nel, A.E., Mädlar, L., Velegol, D., Xia, T., Hoek, E.M.V., Somasundaran, P., Klaessig, F., Castranova, V., Thompson, M., 2009. Understanding biophysicochemical interactions at the nano-bio interface. *Nat. Mater.* 8, 543–557. <https://doi.org/10.1038/nmat2442>.
- O'Brien, D.P., 1987. Description of Escape Responses of Krill (*Crustacea: Euphausiacea*), with Particular Reference to Swarming Behavior and the Size and Proximity of the Predator. *J. Crustac. Biol.* 7, 449–457. <https://doi.org/10.2307/1548294>.
- Obbard, R.W., Sadri, S., Wong, Y.Q., Khitun, A.A., Baker, I., Richard, C., 2014. Global warming releases microplastic legacy frozen in Arctic sea ice. *Earth's Future* 2 (6), 315–320. <https://doi.org/10.1002/2014EF000240>.
- Peeken, I., Primpke, S., Beyer, B., Gütermann, J., Katlein, C., Krumpfen, T., Bergmann, M., Hehmann, L., Gerdts, G., 2018. Arctic sea ice is an important temporal sink and means of transport for microplastic. *Nat. Commun.* 9, 1505. <https://doi.org/10.1038/s41467-018-03825-5>.
- Phillips, R.A., Waluda, C.M., 2020. Albatrosses and petrels at South Georgia as sentinels of marine debris input from vessels in the southwest Atlantic Ocean. *Environ. Int.* 136, 105443. <https://doi.org/10.1016/j.envint.2019.105443>.
- Reed, S., Clark, M., Thompson, R., Hughes, K.A., 2018. Microplastics in marine sediments near Rothera Research Station, Antarctica. *Mar. Pollut. Bull.* 133, 460–463. <https://doi.org/10.1016/j.marpolbul.2018.05.068>.
- Roussel, E.G., Sauvadet, A.L., Allard, J., Chaduteau, C., Richard, P., Bonavita, M.A.C., Chaumillon, E., 2009. Archaeal methane cycling communities associated with gassy subsurface sediments of Marennes-Oléron Bay (France). *Geomicrobiol. J.* 26, 31–43. <https://doi.org/10.1080/01490450802599284>.
- Schirizzi, G.F., Llorca, M., Seró, R., Moyano, E., Barceló, D., Abad, E., Farré, M., 2019. Trace analysis of polystyrene microplastics in natural waters. *Chemosphere* 236. <https://doi.org/10.1016/j.chemosphere.2019.07.052>.
- Schmidt, K., Atkinson, A., 2016. Feeding and food processing in Antarctic krill (*Euphausia superba* Dana). In: Siegel, V. (Ed.), *The Biology and Ecology of Antarctic Krill, Euphausia Superba* Dana. Springer. [https://doi.org/10.1007/978-3-319-29279-3\\_pp\\_1850175-224](https://doi.org/10.1007/978-3-319-29279-3_pp_1850175-224).
- Seear, P., Tarling, G.A., Teschke, M., Meyer, B., Thorne, M.A.S., Clark, M.S., Gatén, E., Rosato, E., 2009. Effects of simulated light regimes on gene expression in Antarctic krill (*Euphausia superba* Dana). *J. Exp. Mar. Biol. Ecol.* 381, 57–64. <https://doi.org/10.1016/j.jembe.2009.09.010>.
- Seear, P.J., Tarling, G.A., Burns, G., Goodall-Copestake, W.P., Gatén, E., Özkaya, Ö., Rosato, E., 2010. Differential gene expression during the moult cycle of Antarctic krill (*Euphausia superba*). *BMC Genomics* 11, 582. <https://doi.org/10.1186/1471-2164-11-582>.
- Sfriso, A.A.A., Tomio, Y., Rosso, B., Gambaro, A., Sfriso, A.A.A., Corami, F., Rastelli, E., Corinaldesi, C., Mistri, M., Munari, C., 2020. Microplastic accumulation in benthic invertebrates in Terra Nova Bay (Ross Sea, Antarctica). *Environ. Int.* 137, 105587. <https://doi.org/10.1016/j.envint.2020.105587>.
- Singh, N., Tiwari, E., Khandelwal, N., Darbha, G.K., 2019. Understanding the stability of nanoplastics in aqueous environments: effect of ionic strength, temperature, dissolved organic matter, clay, and heavy metals. *Environ. Sci. Nano* 6, 2968–2976. <https://doi.org/10.1039/c9en00557a>.
- Suaria, G., Perold, V., Lee, J.R., Lebouard, F., Aliani, S., Ryan, P.G., Sciences, M., Spezia, L., 2020. Floating macro- and microplastics around the Southern Ocean: results from the Antarctic circumnavigation expedition. *Environ. Int.* 136, 105494. <https://doi.org/10.1016/j.envint.2020.105494>.
- Svensen, C., Morata, N., Reigstad, M., 2014. Increased degradation of copepod faecal pellets by co-acting dinoflagellates and *Centropages hamatus*. *Mar. Ecol. Prog. Ser.* 516, 61–70. <https://doi.org/10.3354/meps10976>.
- Svensen, C., Riser, C.W., Reigstad, M., Seuthe, L., 2012. Degradation of copepod faecal pellets in the upper layer: role of microbial community and *Calanus finmarchicus*. *Mar. Ecol. Prog. Ser.* 462, 39–49. <https://doi.org/10.3354/meps09808>.
- Tarling, G.A., Cuzin-Roudy, J., 2008. External parasite infestation depends on moult-frequency and age in Antarctic krill (*Euphausia superba*). *Polar Biol.* 31, 121–130. <https://doi.org/10.1007/s00300-007-0339-2>.
- Tarling, G.A., Fielding, S., 2016. Swarming and behaviour in Antarctic Krill. In: Siegel, V. (Ed.), *Biology and Ecology of Antarctic Krill, Advances in Polar Ecology*. Springer, pp. 279–320.
- Ter Halle, A., Jeanneau, L., Martignac, M., Jardé, E., Pedrono, B., Brach, L., Gigault, J., 2017. Nanoplastic in the North Atlantic Subtropical Gyre. *Environ. Sci. Technol.* 51, 13689–13697. <https://doi.org/10.1021/acs.est.7b03667>.
- Trathan, P.N., Hill, S.L., 2016. The importance of krill predation in the Southern Ocean. In: Siegel, V. (Ed.), *Biology and Ecology of Antarctic Krill, Advances in Polar Ecology*. Springer, pp. 321–350. [https://doi.org/10.1007/978-3-319-29279-3\\_9](https://doi.org/10.1007/978-3-319-29279-3_9).
- Urbaneck, A.K., Rymowicz, W., Strzelecki, M.C., Kociuba, W., Franczak, L., Mironczuk, A.M., 2017. Isolation and characterization of Arctic microorganisms decomposing bioplastics. *AMB Express* 7, 148. <https://doi.org/10.1186/s13568-017-0448-4>.
- Vannuccini, M.L., Grassi, G., Leaver, M.J., Corsi, I., 2016. Combination effects of nano-

- TiO<sub>2</sub> and 2,3,7,8-tetrachlorodibenzo-p-dioxin (TCDD) on biotransformation gene expression in the liver of European sea bass *Dicentrarchus labrax*. *Comp. Biochem. Physiol. Part - C Toxicol. Pharmacol.* 176–177, 71–78. <https://doi.org/10.1016/j.cbpc.2015.07.009>.
- Varó, I., Perini, A., Torreblanca, A., Garcia, Y., Bergami, E., Vannuccini, M.L., Corsi, I., 2019. Time-dependent effects of polystyrene nanoparticles in brine shrimp *Artemia franciscana* at physiological, biochemical and molecular levels. *Sci. Total Environ.* 675, 570–580. <https://doi.org/10.1016/j.scitotenv.2019.04.157>.
- Venâncio, C., Ferreira, I., Martins, M.A., Soares, A.M.V.M., Lopes, I., Oliveira, M., 2019. The effects of nanoplastics on marine plankton: a case study with poly-methylmethacrylate. *Ecotoxicol. Environ. Saf.* 184. <https://doi.org/10.1016/j.ecoenv.2019.109632>.
- Vijver, M.G., Zhai, Y., Wang, Z., Peijnenburg, W.J.G.M., 2018. Emerging investigator series: the dynamics of particle size distributions need to be accounted for in bio-availability modelling of nanoparticles. *Environ. Sci. Nano* 5, 2473–2481. <https://doi.org/10.1039/c8en00572a>.
- Waller, C.L., Grif, H.J., Waluda, C.M., Thorpe, S.E., Loaiza, I., Moreno, B., Pachterres, C.O., Hughes, K.A., 2017. Microplastics in the Antarctic marine system: an emerging area of research. *Sci. Total Environ.* 598, 220–227. <https://doi.org/10.1016/j.scitotenv.2017.03.283>.
- Wieczorek, A.M., Croot, P.L., Lombard, F., Sheahan, J.N., Doyle, T.K., 2019. Microplastic ingestion by gelatinous zooplankton may lower efficiency of the biological pump. *Environ. Sci. Technol.* 53, 5387–5395. <https://doi.org/10.1021/acs.est.8b07174>.
- Yang, Y., Guo, Y., Brien, A.O., Lins, T.F., Rochman, C.M., Sinton, D., 2020. Biological responses to climate change and nanoplastics are altered in concert: full-factorial screening reveals effects of multiple stressors on primary producers. *Environ. Sci. Technol.* 54 (4), 2401–2410. <https://doi.org/10.1021/acs.est.9b07040>.
- Zane, L., Patarnello, T., 2000. Krill: a possible model for investigating the effects of ocean currents on the genetic structure of a pelagic invertebrate. *Can. J. Fish. Aquat. Sci.* 57, 16–23. <https://doi.org/10.1139/f00-166>.
- Zhang, F., Wang, Z., Wang, S., Fang, H., Wang, D., 2019. Aquatic behavior and toxicity of polystyrene nanoplastic particles with different functional groups: complex roles of pH, dissolved organic carbon and divalent cations. *Chemosphere* 228, 195–203. <https://doi.org/10.1016/j.chemosphere.2019.04.115>.